

STIS Near-IR Fringing. II. Basics and Use of Contemporaneous Flats for Spectroscopy of Point Sources (Rev. A)

Paul Goudfrooij, Ralph C. Bohlin, Jeremy R. Walsh, and Stefi A. Baum
May 1998 (Revised November 1998)

ABSTRACT

G750L and G750M spectra of white dwarfs have been analyzed to study the accuracy with which one can correct for long-wavelength fringing on the STIS CCD. Flat-fielding results using pre-flight and in-flight long-slit lamp flats are compared with those using contemporaneous lamp flats (taken during the course of science data collection, in order to keep the same Mode Select Mechanism position as the science spectra). The contemporaneous lamp flats are taken through a short slit to mimic a point source. In the case of G750L spectra, contemporaneous flats are essential if a signal-to-noise above ~ 30 is required in wavelength regions where the fringing is significant ($\sim 700 - 1000$ nm). The residuals of the fringes in G750L spectra can be reduced to below the 1% level by division by a well-exposed contemporaneous fringe flat taken through a short slit. The superiority of contemporaneous short-slit flats over long-slit flats is somewhat less critical for G750M spectra, but still quite significant. For the G750M case, contemporaneous fringe flats are essential to reach signal-to-noise ratios above ~ 50 . The effects of on-orbit thermal drifts are evaluated and corrected for by matching the fringe pattern of star and flat along the dispersion direction. The influence of the red 'halo' (scattered light) to the tungsten fringe flats is corrected for by scaling the amplitude of the fringes. In this revision we provide an updated recommendation for obtaining fringe flats along with 52x0.2F1 slit spectra (see Table 2).

1. Introduction

The thinned, backside-illuminated SITe CCD used in STIS is thin enough to exhibit significant fringing at wavelengths longward of ~ 700 nm, which limits the signal-to-noise obtainable in the majority of the wavelength settings of the G750L and G750M gratings. Briefly, the fringes are caused by interference of multiple reflections between the two surfaces of the CCD, in case the distance between the surfaces is a small integer multiple of

the wavelength of the incident light. The fringe pattern at a given position on the CCD is a convolution of the local distance between the front and back surfaces of the CCD and the wavelength incident on that particular position. Thus the fringe pattern for low- and high-resolution data differ significantly in appearance. STIS Instrument Science Report (hereinafter ISR) 97-16 [which deals with fringing in spectra of extended sources] contains a somewhat more detailed explanation of the physics of the fringe process. Below we consider the fringe patterns for G750L (low-resolution) and G750M (medium-resolution) spectra separately, taking into account issues relevant to the in-flight behavior of the spectroscopic modes of STIS.

1.1. Fringing in G750L spectra

1.1.1. G750L Fringe Morphology

In the case of G750L spectra, the morphology of the fringing pattern is governed by the fact that wavelength changes rapidly from one X-pixel position to the next. The contours of constant wavelength are therefore almost vertical (i.e., parallel to the slit), and hence so are the fringes. Fig. 1 is a G750L flat field image, taken with the 52x0.1 slit at a central wavelength of 775.1 nm. The large variation in lamp brightness across the spectral range has been removed by fitting a cubic spline through the data [cf. Section 3.3] and dividing the result into each row. Fig. 1 shows that the fringes are tilted slightly with respect to the Y-axis, which is due to the fact that the surfaces of the CCD are not exactly parallel. The fringe amplitude increases from the blue (left) part of the image towards the red. Table 1 provides the peak-to-peak and RMS amplitudes of the fringes as a function of wavelength. Blueward of 700 nm, the fringe amplitude is of the order of or less than the photon counting statistics.

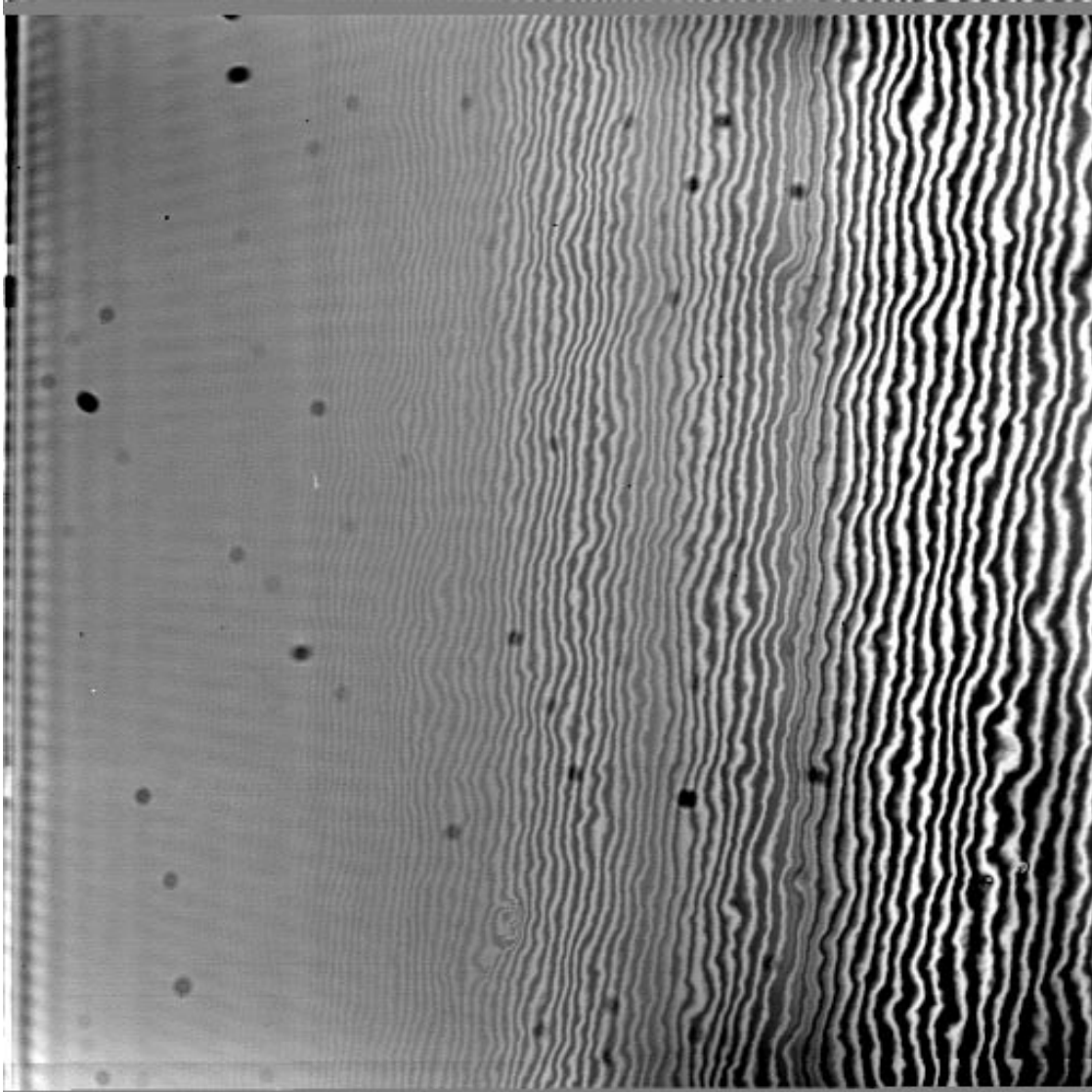
1.1.2. On Correction Accuracy for G750L Fringing

1. Shifts Between Science Exposures and Fringe Flats

Tests on STIS pre-flight (ground calibration) data have shown that if a library of G750L “fringe flats” is available, a given fringe flat can be shifted to reduce the fringe amplitude of a given observation from about 25% to about 5% provided that the wavelength settings of fringe flat and science observation are within about 3 pixels. However, the combined effects of the non-repeatability of the Mode Select Mechanism (hereinafter MSM) of STIS and on-orbit thermal drifts can amount to shifts larger than this. Thus, it is clear that a substantial library of fringe flats is required to ensure a successful fringe correction¹. Alternatively, a fringe flat should be taken at the same MSM position as the science data (a “contemporaneous flat”) to ensure the smallest possible shift between fringe flat and science spectrum. STIS ISR 97-16 describes the benefits of using contem-

poraneous fringe flats for de-fringing extended sources, while we describe the use of contemporaneous flats for point-source de-fringing in this ISR.

Figure 1: STIS CCD Fringe flat (tungsten lamp exposure of which the large-scale trend with wavelength is removed) for the G750L grating. the central wavelength is 775.1 nm and wavelength increases towards the right.



2. External vs. Internal Illumination

A potential further complication in using fringe flats to correct science data is that the fringe flats are taken with an internal lamp while the scientific data are from an external

1. We are currently building up a library of G750L fringe flats by means of Cycle 7 Calibration Program No. 7711 and from contemporaneous fringe flats (cf. below). This library is not expected to be available soon, however. We recommend observers to take contemporaneous flats instead (see below).

object. The light paths are slightly different, and so are the focal ratios of the two beams. To evaluate how well the internal lamp could be used to correct science data, a series of exposures was taken during ground calibration with the internal lamp and an external lamp in successive exposures, without moving the MSM. The analysis of the G750L spectra (central wavelength 775.1 nm) showed residuals in the ratio of the internal to the external spectrum of about 3% over the last 200 pixels (or wavelengths above 930 nm), and somewhat lower from pixel 600 to pixel 800 (~ 820 - 930 nm); the RMS residual over the entire range (820 - 1025 nm) was just under 1%. This would suggest a priori that G750L fringes might not be removable to a much better accuracy than 1-2% (cf. STIS ISR 97-16).

3. Fringes in Point Source Spectra vs. Fringe Flats: Scattered Light Problems

The amount of scattered light in point source spectra is significantly different from that in diffuse fringe flats (taken with the internal lamp). The STIS CCD features a substantial halo in the red part of the spectrum, 'leaking' light from one row of the CCD into adjacent rows. This adds a pedestal to the lamp flat which is wavelength dependent, and virtually absent in point source spectra. Furthermore, the difference in scattered light between a given external source spectrum and the lamp flat may be dependent on the actual Spectral Energy Distribution (hereinafter SED) of the external source (i.e., the difference of the SEDs of the external source and the lamp). The severity of this problem is a function of external source structure, being most prominent for point sources.

The effect of this pedestal in the fringe flats is to *reduce the amplitude of the fringes in the fringe flat with respect to those in an observed point source spectrum*. The actual effect of scattered light on the results of fringe correction for point source spectra will be discussed in Section 3.5.

1.2. Fringing in G750M spectra

1.2.1. G750M Fringe Morphology

In the case of G750M spectra, the wavelength changes only very slowly with X-pixel position, so that the fringes are expected to be running along a certain angle with respect to the dispersion direction, governed by the shape (degree of planarity) of the CCD. Figure 2 shows a (pre-flight) G750M flat taken with the 52x0.1 slit at a central wavelength of 985.1 nm. Irregular, broad fringes are found to run rather wildly through the image without much sign of coherence; upon initial eye contact, Escher or Mandelbrot would most likely turn the page quickly without any further ado :-). Table 1 lists the G750M fringe amplitude as a function of wavelength.

1.2.2. On Correction Accuracy for G750M Fringing

1. Shifts Between Science Exposures and Fringe Flats

For the G750M case, the situation is somewhat more optimistic. Fringe flats taken during ground calibration showed that if a library of fringe flats were to be built up at wavelength positions spaced about 3 pixels apart, one would be able to correct the fringes to better than 1.5% by using a high S/N fringe flat shifted by at most 1.5 pixels, while shifts of less than 1 pixel would result in a correction better than to within 1%. Again, a library of fringe flats would make defringing life less complicated, while contemporaneous flats will ensure the smallest possible shift between fringe flat and science spectrum.

Table 1. Fringing as a function of wavelength for G750L and G750M flats. The RMS values at short wavelengths give a good indication of the counting statistics in the flats used for this analysis.

| Wavelength (nm) | G750M peak-to-peak | G750M RMS | G750L peak-to-peak | G750L RMS |
|--------------------|-----------------------|--------------|-----------------------|--------------|
| 575.0 | | 1.13 | | |
| 610.0 | | 1.21 | | |
| 660.0 | | 1.23 | | |
| 675.0 | | 1.29 | | |
| 725.0 | 4.62 | 1.52 | 3.18 | 2.13 |
| 775.0 | 9.61 | 3.10 | 8.58 | 3.08 |
| 825.0 | 10.53 | 3.26 | 6.76 | 2.80 |
| 875.0 | 14.83 | 3.85 | 10.81 | 3.98 |
| 925.0 | 27.16 | 9.00 | 23.42 | 7.92 |
| 975.0 | 32.09 | 10.78 | 25.35 | 8.96 |
| 1025.0 | 18.23 | 6.04 | 17.30 | 5.89 |
| 1075.0 | 15.93 | 4.30 | 6.99 | 7.40 |

2. External vs. Internal Illumination

As to the issue of the different illumination from external sources with respect to the internal flats, the G750M ground-based spectra showed very similar fringe patterns from both the external and the internal lamps. The results were consistent with no residual fringing in excess of the photon counting statistics.

3. Fringes in Point Source Spectra vs. Fringe Flats: Scattered Light Problems

The issue of the pedestal introduced by the red halo in fringe flats is present in G750M as well as in G750L spectra (see above). The effect of this pedestal to the amplitude of the fringes in the flats relative to those in the source spectrum is, however, expected to be much smaller than in the G750L case, since the fringes in G750M spectra are neither per-

pendicular to the dispersion nor as closely spaced as those in G750L spectra (cf. Figs. 1 and 2).

1.3. Strategy for Resolving the Fringing Problem

A potential way to significantly reduce the scattered light problem for long slit spectra of point sources is to take fringe flats through a short slit which is concentric with the long slit used for the science exposures, since the structure of such flats should mimic a PSF much more accurately than the long slits [these short slits are normally used for echelle spectroscopy]. The slits supported for science with the G750L and G750M gratings and the associated slits to use for fringe flats in the case of point source observations in the near-IR are listed in Table 2 (cf. also STIS ISR 97-15). Note that while the short slits are concentric with the long slits in the direction perpendicular to the dispersion, there is a small intrinsic shift (of order 0.1-0.6 pixel) between the long and short slits along the dispersion, which has to be corrected for (cf. Section 3.4).

Table 2. Short-slit Fringe Flats to be used for Point Source observations.

| Supported Science Slit | Fringe Flat Slit(s) | Intrinsic spectral shift between science and fringe flat slit (pixels) |
|------------------------|-----------------------------|--|
| 52x2 | 0.3x0.09 | 0.35 |
| 52x0.5 | 0.3x0.09 | 0.44 |
| 52x0.2 | 0.3x0.09 | 0.58 |
| 52x0.2F1 | 0.3x0.09 AND 52x0.2F1 | 0.58 0.00 |
| 52x0.1 | 0.2x0.06 | 0.12 |

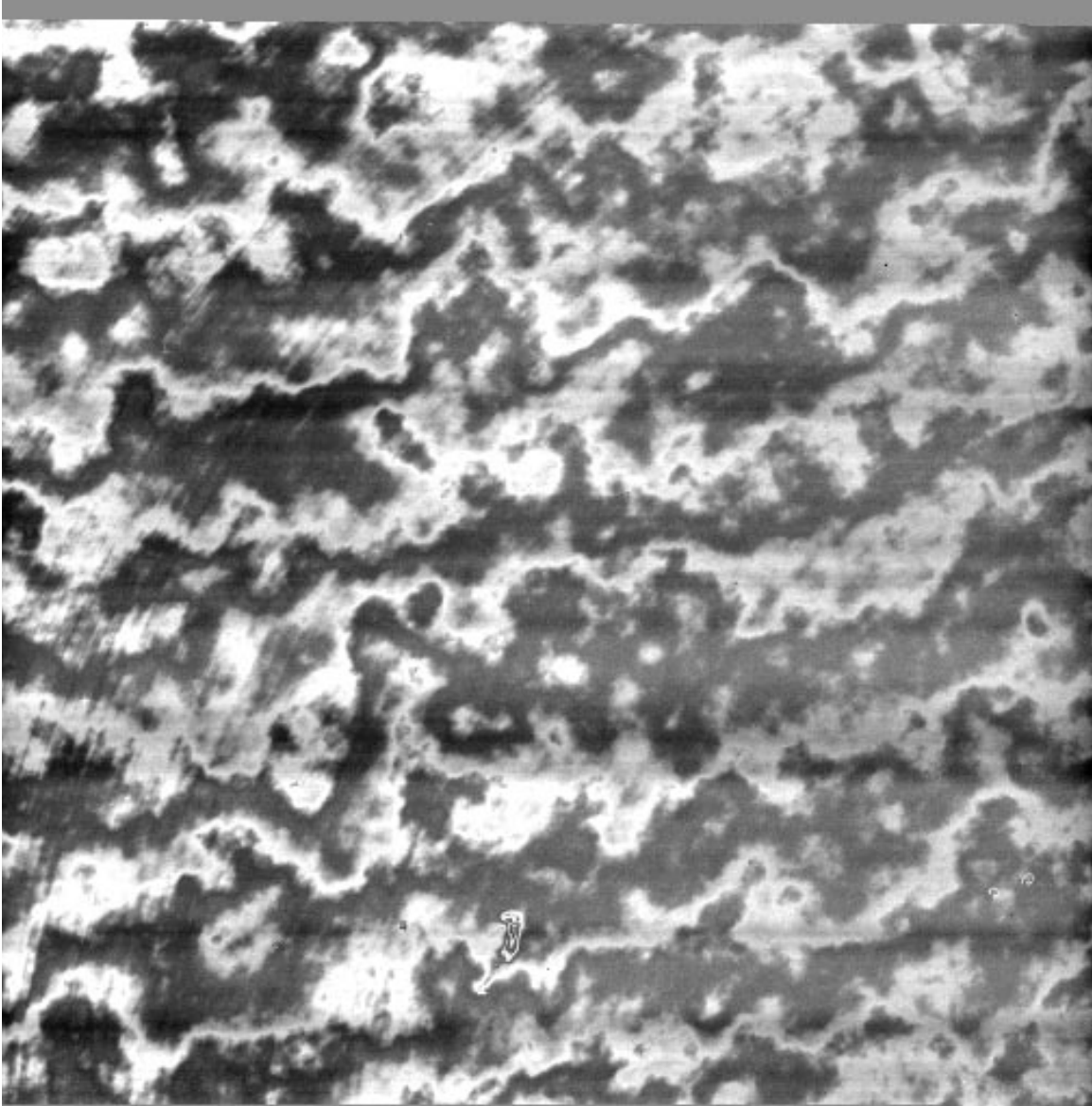
A few notes are of importance on the use of short-slit flats:

1. *Note that fringe removal for point sources that are offset (in the spatial direction) from the center of the long slit is not possible with a short-slit flat; one has to use long-slit flats for those.*
2. *The length of the short slits used for these contemporaneous flats (0.2 - 0.3 arcsec) does not allow one to sample the full PSF, especially in the cases of (i) spectra taken with the 52x0.1 slit, in which case the short-slit fringe flat only covers 0.2 arcsec in the spatial direction, and (ii) spectra taken with the 52x0.2F1 slit. We recommend to obtain a long-slit fringe flat as well in those cases.*

Calibration proposals were designed and implemented to test how well fringes can be removed from near-IR spectra of both extended objects and point sources, by means of

contemporaneous flats. The initial tests on spectra of extended objects are described in STIS ISR 97-16, while we describe the tests on spectra of point sources in this ISR.

Figure 2: STIS CCD Fringe flat for the G750M grating. The central wavelength is 985.1 nm and wavelength increases to the right.



2. Observations

Contemporaneous G750L short-slit flats were implemented in three visits of SMOV proposal 7063 (STIS CCD Contamination Monitor), and contemporaneous G750M short-slit flat were implemented in several visits of Cycle 7 proposal 7656 (STIS Spectroscopic and Imaging Sensitivity, CCD). The targets were white dwarfs GD 153 and BD+75°325.

The slit for the ‘science’ exposures was the 52x2 slit, and the contemporaneous flats were taken with the 0.3x0.09 slit. Table 3 lists other details about the observations, including counting statistics for the star spectra and the fringe flats. Prior to the star observations, a target acquisition was made with the F28x50OII filter. All the observations were made with no binning, in CCDGAIN=4. The GD153 spectra were CR-SPLIT 4, and the BD+75°325 spectra were CR-SPLIT 2. The tungsten lamp exposures were not CR-SPLIT, but instead specified as “Number_Of_Iterations=2” in the RPS2 file. It should be noted that the tungsten lamp exposures were made with only one bulb on, whereas fringe flats are currently taken with two bulbs being on. Observers are referred to STIS ISR 97-15 for up-to-date exposure-time recommendations for GO-added contemporaneous flats.

Table 3. Observational Details. Column 7 (“Mean Count”) lists the total intensity of the star spectrum, integrated over 11 rows perpendicular to the dispersion, and averaged over the wavelength region where fringing is an issue and no significant absorption lines are seen [700-950 nm for the G750L spectra, 770-800 nm for the G750M spectra]. For the tungsten fringe flats, we list the mean count *per row* over the same wavelength range.

| Target | Grating, CENWAVE | Date of Observation | UT | Dataset Name | Exp. time (s) | Mean Count (e ⁻) |
|-----------|---------------------|------------------------|----------|-----------------|------------------|---------------------------------|
| Tungsten | G750L, 7751 | Jun 18, 1997 | 05:19:04 | o3tt46030 | 240 | 16800 |
| GD 153 | „ | „ | 05:46:23 | o3tt46040 | 2282 | 27530 |
| Tungsten | „ | Jun 25, 1997 | 05:00:42 | o3tt47030 | 240 | 16852 |
| GD 153 | „ | „ | 05:31:49 | o3tt47040 | 2282 | 27548 |
| Tungsten | „ | Jul 01, 1997 | 12:29:07 | o3tt48030 | 240 | 16848 |
| GD 153 | „ | „ | 13:11:51 | o3tt48040 | 2282 | 27596 |
| BD+75°325 | G750M, 7795 | Oct 13, 1997 | 19:25:03 | o4a505080 | 72 | 29836 |
| Tungsten | „ | „ | 19:29:10 | o4a505090 | 240 | 8823 |

3. Data Analysis: Reduction of Fringe Flats

3.1. IRAF *cl* Tasks for Fringe Flat Analysis

The whole data reduction procedure described below is supported by four tasks in the `stdas.hst_calib.stis` package within IRAF: `normspflat`, `prepspec`, `mkfringeplat` and `defringe`². Flow charts and tutorials on the use of these three scripts are provided in a separate, forthcoming ISR. *These tasks are useful for de-fringing spectra of extended sources as well as spectra of point sources.*

2. At the time this report is issued, these scripts are scheduled to be installed in the `stdas.hst_calib.stis` package within STSDAS in May 1998.

3.2. Initial Processing

The raw contemporaneous fringe flats have to be debiased, corrected for cosmic rays, and dark subtracted. These basic steps are most conveniently done with CALSTIS [modules `basic2d` and `ocreject`, available within STSDAS], which also takes care of hot pixel removal [be sure in this respect to retrieve the latest dark reference file with `USEAFTER` date just before the observation date]. Fringe flats will be undergoing shifting and scaling procedures prior to their final use, so that they are not suited for correcting pixel-to-pixel variations of the CCD. It is therefore important to divide the dark-subtracted flat by another ‘pixel-to-pixel’ flat [that does *not* exhibit any fringing]. A good choice for a pixel-to-pixel flat is the 50CCD mode flat field [currently `h4s13511o_pfl.fits`], which is the one we used³. In the context of CALSTIS, this step is done by setting the `PFLTFILE` keyword in the main header of the fringe flat to the appropriate fits file, e.g.,

```
cl> hedit fringeflat.fits[0] PFLTFILE h4s13511o_pfl.fits4
```

3.3. Fitting the Lamp Function

The lamp function is the response of STIS to the spectral energy distribution of the tungsten lamp, and removing it from the fringe flat is the most tedious step of the reduction. Note that this step potentially affects absolute flux calibration, as the sensitivity curves for STIS gratings have been derived using independent fits to the lamp function which utilize a different algorithm. The lamp functions of G750L and G750M spectra can be recognized in Fig. 3 as the global shape of the lamp spectra.

We have been able to produce adequate fits to the lamp function by using cubic splines by means of the `images.imfit.fit1d` task, available within IRAF. Due to the sensitivity curves of the STIS instrument components, the number of spline pieces to be used to obtain an adequate fit is dependent on the grating and the wavelength setting. Table 4 lists the number of spline pieces used for the different settings.

Table 4. Spline Fit Characteristics for the Different Wavelength Settings

| Grating | CENWAVE | Number of Spline Pieces [ORDER] |
|---------|-------------|---|
| G750L | 7751 | Composite ^a of two fits: ORDER=60 and ORDER=12 |
| G750M | All < 9851 | ORDER = 1 |
| G750M | 9851, 10363 | ORDER = 2 |

a. The exact way in which the composite fit is derived will be reported in the forthcoming ISR which will contain a tutorial for use of the fringe flat scripts.

3. For this purpose, we recommend observers to retrieve the latest 50CCD flat from the archive.
4. Note that this pixel-to-pixel flat also has to be specified as `PFLTFILE` for the science observations. this is done by means of the fringe flat tasks within STSDAS.

Figure 3: Spectral Energy Distributions of lamp fringe flats: (a, upper) taken with the G750L grating at a central wavelength of 775.1 nm, and (b, lower) taken with the G750M grating at a central wavelength of 779.5 nm. The thick solid lines depict the spline fits to the lamp function.

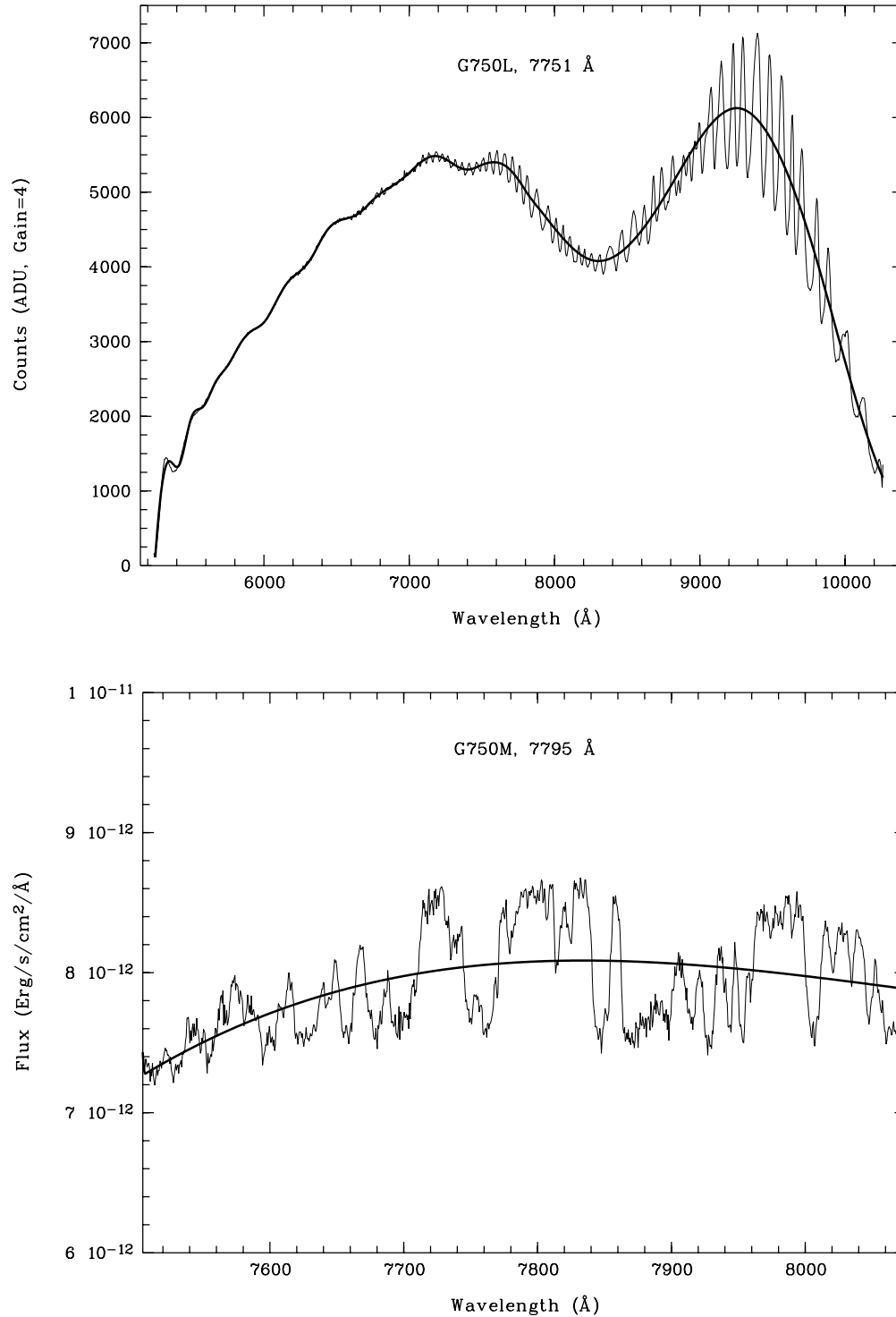
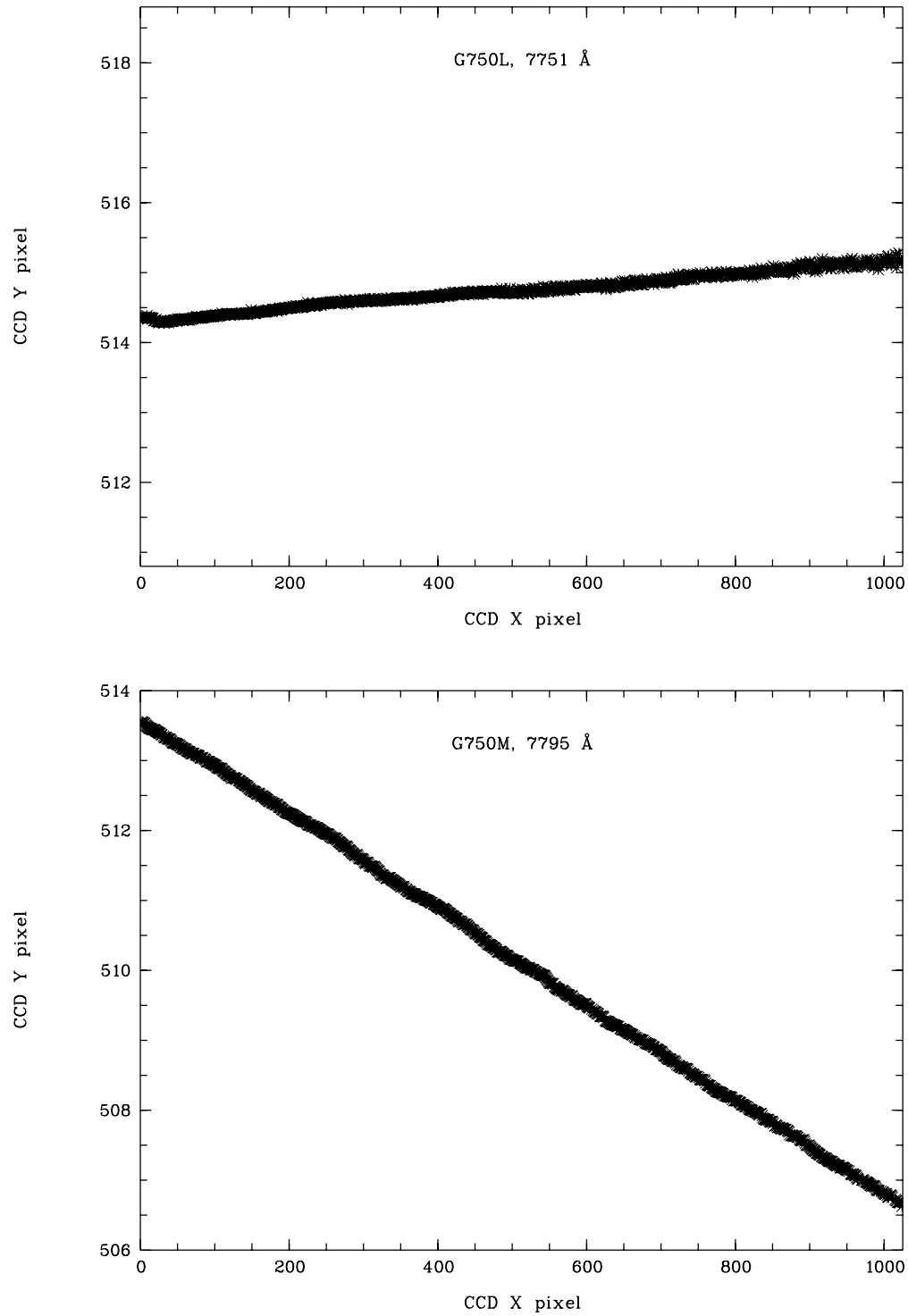


Figure 4: Centroid of a star as a function of wavelength for (a, upper) the G750L grating at a central wavelength of 775.1 nm, and (b, lower) the G750M grating at a central wavelength of 779.5 nm. Notice the significant tilt of the G750M spectrum.



The actual fitting of the lamp function for short-slit fringe flats was done line-by-line on the `_cr j.fits` files [cosmic-ray-rejected, pixel-to-pixel-corrected] for the G750L case and on the `_sx2.fits` files [wavelength-calibrated, corrected for tilt and geometric distortion] for the G750M case. The reason for this difference is that G750M spectra are dispersed along a skewed angle with respect to the CCD rows, amounting to a difference of ~ 8 pixels (peak-to-peak) from the short- to the long-wavelength end of the spectrum. Since the short slits are only 4-8 CCD pixels long, the G750M spectra have to be geometrically corrected prior to fitting the lamp function. In contrast, the geometric distortion of the G750L spectra is very small: less than 1 pixel total. The grating tilt (and the geometric distortion) near the center of the slit are depicted in Fig. 4 which shows the centroids of a point source as a function of wavelength for both G750L and G750M spectra.

3.4. Shifting the Fringe Flat to Match the Fringe Pattern of the Star Spectrum

After removal of the lamp function, the fringe flat will have to be aligned with the fringes in the point source spectrum to compensate for the intrinsic offset introduced by the use of a different slit (cf. Table 2) and on-orbit thermal drifts. The typical shift is a few tenths of a pixel for contemporaneous fringe flats, but can amount to several pixels when using library fringe flats due to the non-repeatability of the MSM (cf. Section 1.1.2). One way of accomplishing this is to perform a cross correlation between an extracted star spectrum normalized by its continuum and the fringe flat extracted over the same image lines, e.g. by means of the IRAF task `stdas.hst_calib.ctools.poffset`, which is generally found to achieve good results in this respect. However, in the context of our STSDAS task `mkfringeflat` [to be made available in `stdas.hst_calib.stis`], we have chosen to implement an empirical way to find the best shift which ensures a somewhat higher level of control over the solution found: After shifting the fringe flat by discrete steps (of which the increment and total range are user-specified) along the dispersion, the star spectrum is divided by the shifted flat and the variance of the flatfielded star spectrum is measured. From the shifts that deliver the 5 lowest variance values (centered on the shift delivering the lowest variance), a weighted average shift is calculated and applied to the fringe flat⁵. The task allows for optimizing the shift for a specific range in wavelength which may be helpful in case e.g., strong narrow emission lines are present in the science spectrum.

Appropriate ranges and increments for finding the right shift with the `mkfringeflat` task are:

For contemporaneous flats: from -0.5 to 0.5, increment 0.1;

For library flats: from -3 to 3, increment 0.5, followed by a run with smaller increment centered on the best shift from the first run.

5. if the shift delivering the lowest variance is only one step away from either extremum of the shift range, then the 3 lowest variance values are used in the weighting procedure.

The effect of the shift along the dispersion to the resulting fringe correction for a G750L white dwarf spectrum is shown in Fig. 5. Results of using the pipeline (pre-flight) flat and the contemporaneous fringe flat are shown, as well as the “raw” spectrum (i.e., the spectrum prior to the fringe correction) for comparison. Fig. 6 is a similar plot for the G750M case. The spectra shown in Figs. 5 and 6 were produced by adding 7 rows centered on the star. It is clear that the improvement in fringe correction resulting from the use of contemporaneous flats is marked, especially for the G750L spectra. The improvement resulting from the shifting procedure is also significant in the case of G750L spectra, especially when using the pipeline flat which needed a shift of 2.4 pixels, but less so for the G750M case. This difference is mainly due to the difference in dispersion (and its effect on fringing), as discussed in Section 1. Table 5 lists the RMSs of the fringe residuals in the final, normalized, de-fringed spectra before and after applying the shift. They were derived in the wavelength region void of obvious spectral lines: 700-950 nm for the G750L spectra, and 770-800 nm for the G750M spectra. The longer wavelengths were not included because the stellar signal is low so that photon noise dominates there.

3.5. Correction for Scattered Light: Scaling the Fringe Amplitude

To remove the influence of scattered light from the fringe flats (cf. Sections 1.1.2 and 1.2.2), we scaled the amplitude of the fringes in the shifted fringe flat by a [user-specified] range of multiplicative scale factors prior to applying them as fringe flat to find the lowest variance in the resulting de-fringed point source spectrum, using the same empirical method as described above in Section 3.4 for the determination of the shift. The results of this scattered light correction are depicted in Figs. 7 and 8 for the G750L and G750M spectra, respectively, and listed in Table 5.

The correction for scattered light improves the fringe removal, especially in the case when long-slit flats are used (where the correction is substantial, as expected). Short-slit contemporaneous flats are also found to benefit from the scattered light correction, cf. Table 5, even though the corrections to the fringe flats are smaller. As predicted in Section 1.2.2, the corrections to the fringe amplitudes are much smaller for the G750M spectra than those for the G750L spectra (cf. Figs. 7 and 8).

Appropriate ranges and increments for finding the optimal multiplicative scale factor with the `mkfringe` task are (typical values; a given flat may need slightly different values):

For contemporaneous flats: from 0.8 to 1.2, increment 0.05;

For library flats: from 0.9 to 1.3, increment 0.05.

Figure 5: The effect of shifting the fringe flat prior to its application to the white dwarf G750L spectrum. The upper spectrum shows the star spectrum without any flat field correction. The second spectrum is the result of de-fringing the star spectrum with the standard [pre-flight, long-slit] pipeline flat; the third spectrum has been de-fringed with the pipeline flat after applying a shift of 2.4 pixels along the dispersion. The fourth spectrum is the result of de-fringing with the contemporaneous flat, and the fifth spectrum was de-fringed with the contemporaneous flat after applying a shift of 0.18 pixels along the dispersion. All spectra were divided by a smooth spline fit to the stellar continuum.

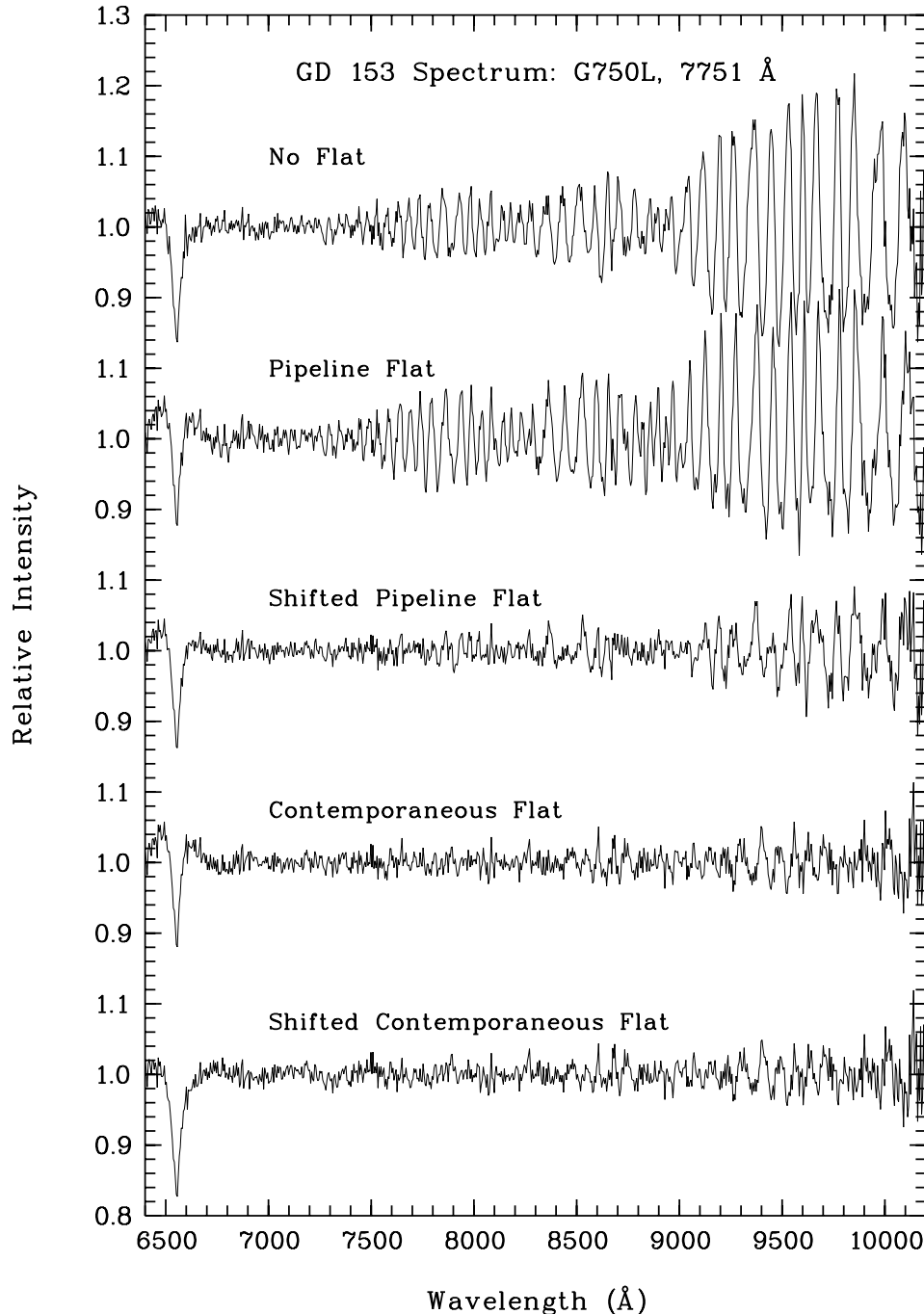


Figure 6: Similar to Fig. 5, but now for the G750M case. The required shifts to the pipeline (long-slit) flat and the contemporaneous flat along the dispersion were 0.5 and 0.44 pixels, respectively.

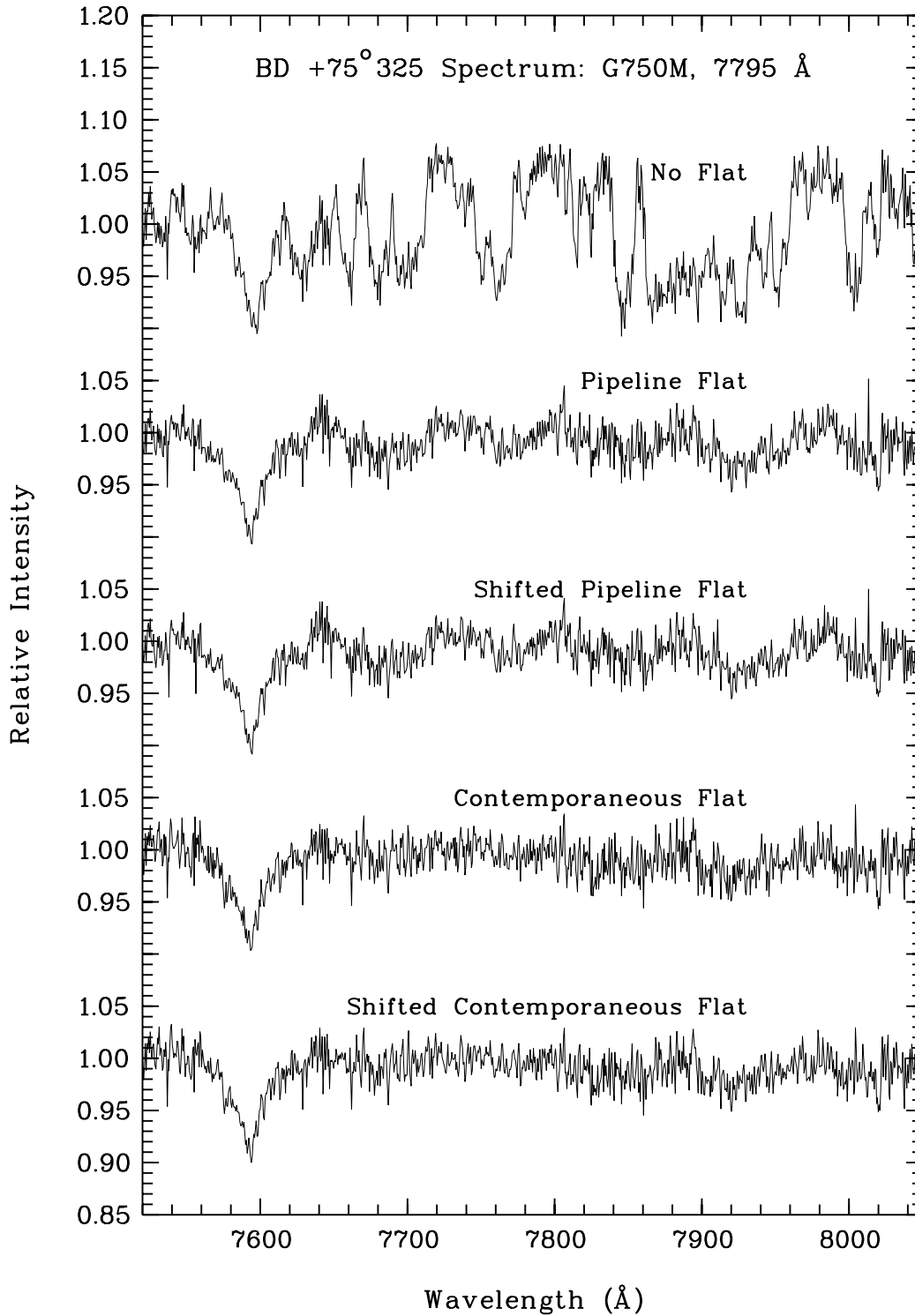


Figure 7: The effect of scaling the amplitude of the fringes in the fringe flat prior to its application to the white dwarf G750L spectrum. The upper spectrum shows the result of de-fringing with the shifted long-slit pipeline flat (cf. Fig. 5). The second spectrum shows the result of de-fringing with the shifted pipeline flat after having scaled the fringe amplitude by a factor 1.26. The third spectrum was de-fringed with the shifted contemporaneous flat (cf. Fig. 5), and the fourth spectrum was de-fringed with the shifted contemporaneous flat after having scaled the fringe amplitude by a factor 0.89.

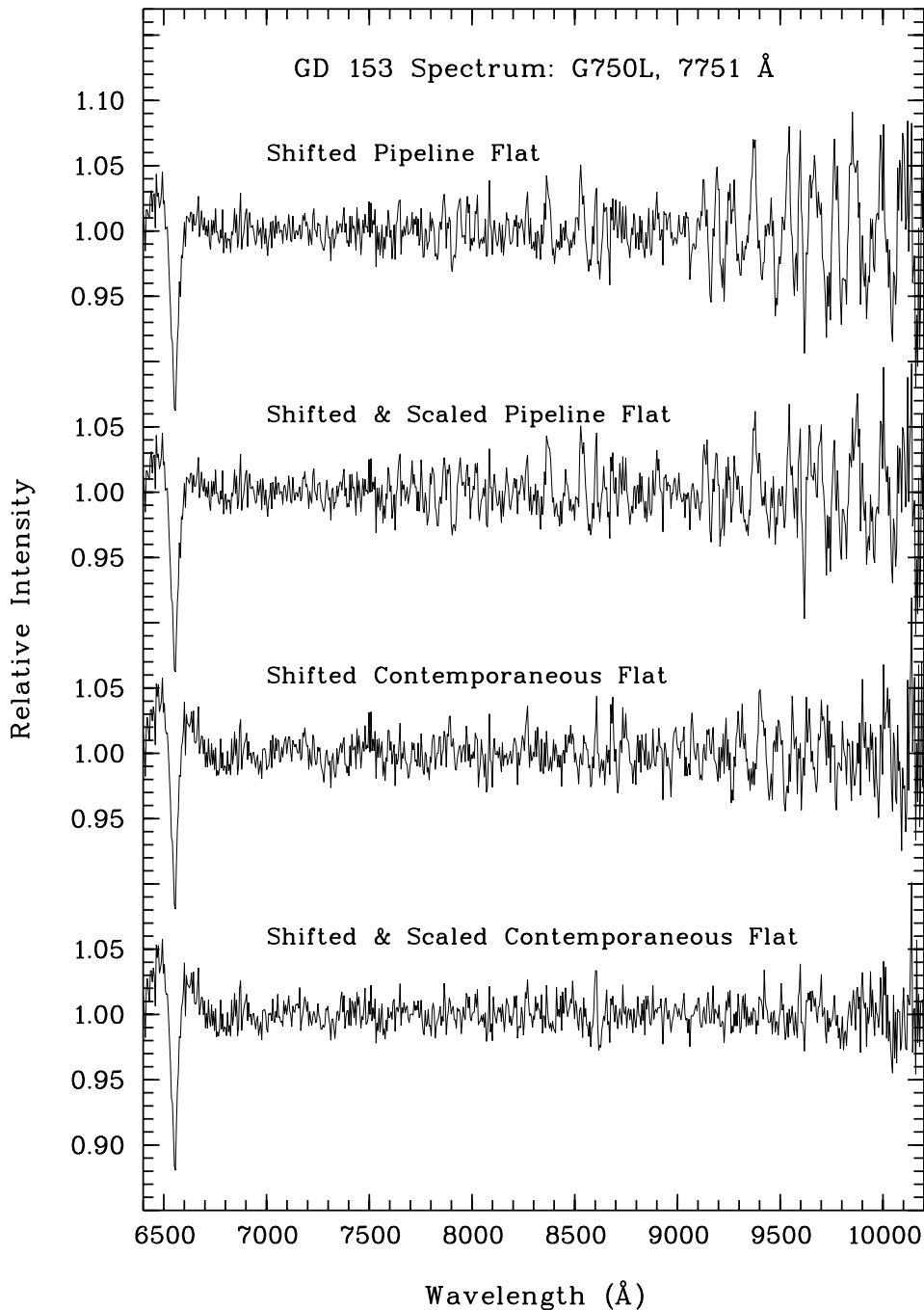


Figure 8: Similar to Fig. 7, but now for the G750M case. The scaling factors for the shifted pipeline flat and the shifted contemporaneous flat were 1.08 and 1.02, respectively.

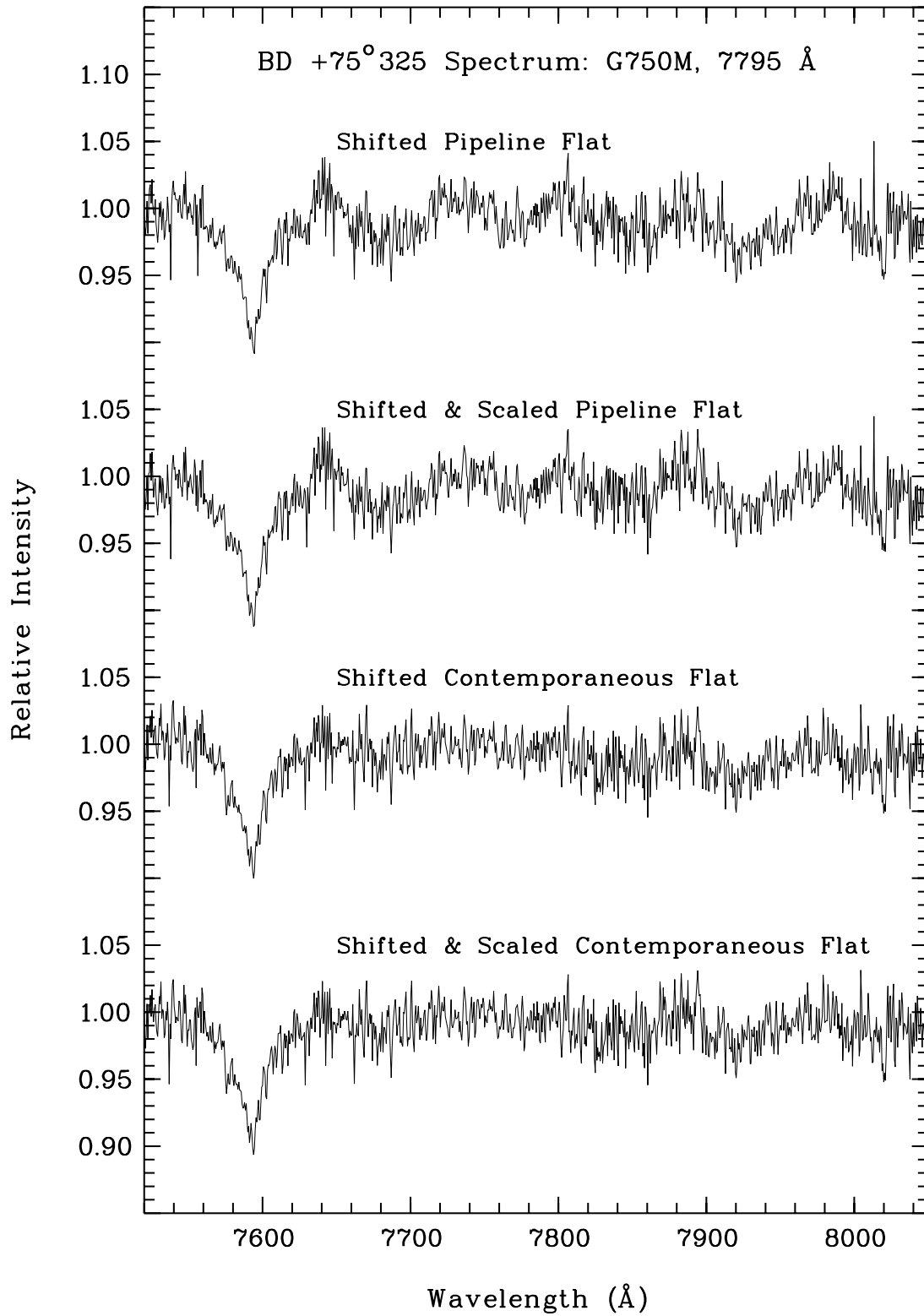


Table 5. RMS Values (in %; for 700-950 nm for the G750L spectra and 770-800 nm for the G750M spectra) after Fringe Correction: Contemporaneous vs. Pipeline Long-slit Flat. The results for the G750L spectra are the average of the G750L datasets listed in Table 3.

| White Dwarf Spectrum | Pipeline flat | Shifted Pipeline flat | Shifted & scaled pipeline flat | Contemp. flat | Shifted contemp. flat | Shifted & scaled contemp. flat | Poisson limit of contemp. flat |
|----------------------|---------------|-----------------------|--------------------------------|---------------|-----------------------|--------------------------------|--------------------------------|
| G750L / 7721 | 4.94 | 1.75 | 1.59 | 1.24 | 1.23 | 0.95 | 0.77 |
| G750M / 7795 | 1.65 | 1.64 | 1.56 | 1.58 | 1.47 | 1.42 | 1.10 |

4. Conclusions and Recommendations

1. For G750L spectra of point sources, contemporaneous fringe flats are essential if exploitation of the data at wavelengths above 750 nm at signal-to-noise ratios exceeding ~ 30 is required. We recommend that contemporaneous flats be obtained routinely with all G750L observations. For point sources, short-slit flats are found to provide a significantly better fringe correction than do long-slit flats.
2. For G750M spectra of point sources, contemporaneous fringe flats are essential if exploitation of the data at wavelengths above 750 nm at signal-to-noise ratios exceeding ~ 60 is required. We recommend that contemporaneous flats be obtained routinely with all G750M observations. For point sources, short-slit flats are found to provide a significantly better fringe correction than do long-slit flats.
3. The highest signal-to-noise values attainable after defringing point source spectra with contemporaneous flats are slightly over 100 per pixel for G750L spectra, and about 70 per pixel for G750M spectra. The latter number was somewhat limited by the photon noise in the G750M contemporaneous flats used in this study. When the G750M fringe flats are taken with sufficient counting statistics, we expect to yield signal-to-noise values comparable with those of G750L spectra.
4. Four STSDAS scripts: `normspflat`, `prepspec`, `mkfringe` and `defringe` have been created to aid the observer in creating the best fringe flat from contemporaneous (or library) flats, and applying it to the science spectra. These scripts are designed to be applied to both short-slit flats (for spectra of point sources) and long-slit flats (for spectra of extended sources). An ISR which includes a tutorial on the use of these tasks is forthcoming.

5. Acknowledgements

It is a pleasure to acknowledge Eliot Malamuth's work on the pre-flight calibration of long-wavelength fringes (cf. STIS IDT Pre-Launch Analysis Report No. 85). We also acknowledge useful discussions with Phil Plait (cf. STIS IDT Post-Launch Analysis Report No. 26).